Nanoscale

PAPER

View Article Online
View Journal | View Issue

Cite this: *Nanoscale*, 2024, **16**, 15615

Facile roll-to-roll production of nanoporous fiber coatings for advanced wound care sutures†

Tavia Walsh, [a,b] Zhina Hadisi,[a,b] Seyed Mohammad Hossein Dabiri,[a,b] Sadegh Hasanpour,[a,b] Sadaf Samimi,[a,b] Mostafa Azimzadeh[a,b] and Mohsen Akbari *[a,b]

Theranostic sutures are derived from innovative ideas to enhance wound healing results by adding wound diagnostics and therapeutics to typical sutures by functionalizing them with additional materials. Here, we present a new direct electrospinning method for the fast, continuous, inexpensive, and high-throughput production of versatile nanofibrous-coated suture threads, with precise control over various essential microstructural and physical characteristics. The thickness of the coating layer and the alignment of nanofibers with the thread's direction can be adjusted by the user by varying the spooling speed and the displacement between the spinneret needle and thread. To show the flexibility of our method for a range of different materials selected, gelatin, polycaprolactone, silk fibroin, and PEDOT:PSS (poly(3,4-ethylene dioxythiophene):poly(styrene sulfonate)) were the resultant nanofibers characterized by scanning electron microscopy (SEM) imaging and conductivity tests. In a series of *in vitro* and *ex vivo* tests (pig skin), sutures were successfully tested for their flexibility and mechanical properties when used as weaving and knotting sutures, and their biocompatibility with a keratinocyte cell line. For temperature-based drug-releasing tests, two fluorescent molecules as drug models with high and low molecular weight, namely fluorescein isothiocyanate-dextran (20 kDa) and rhodamine B (470 Da), were used, and their steady release with incremental increase of temperature to 37 °C over 120 min was seen, which is appropriate for bacterial treatment drugs. Given the advantages of the presented technique, it seems to have promising potential to be used in future medical applications for wound closure and bacterial infection treatment *via* a temperature-triggered drug release strategy.

Received 1st April 2024,
Accepted 22nd July 2024

DOI: 10.1039/d4nr01432d

rsc.li/nanoscale

1. Introduction

Sutures have been traditionally used to close wounds resulting from trauma or surgery by bringing the edges of the wound together.[1] To effectively seal or heal, sutures possess robust knotting capabilities, minimum stress during insertion, high tensile strength, low risk of infection, excellent biocompatibility, and minimal biotoxicity following biodegradation.[2] In the context of complex wound healing, sutures may be used to administer medicine directly to the wound site at specific times to prevent infection or promote healing.[3] Moreover, the integration of electroconductive materials into suture structures has facilitated the development of biosensing capabilities through small, flexible systems that can be seamlessly incorporated into wounds.[4–8] All in all, sutures serve as indispensable tools in wound closure, offering not only mechanical strength and flexibility but also the potential for targeted medication delivery and advanced biosensing capabilities, thus contributing to enhanced patient care and improved clinical outcomes.[9]

Sutures are produced through various methods to meet specific clinical needs and preferences. The most common method involves extruding synthetic polymers like polyglycolic acid (PGA), polylactic acid (PLA), or polydioxanone (PDO) into monofilament or multifilament threads, which are then twisted or braided to enhance tensile strength and handling properties.[10,11] Monofilament sutures offer reduced tissue drag and a smoother surface for reduced bacterial adhesion, while multifilament sutures provide greater flexibility and knot security.[12] Additionally, absorbable sutures are manufactured by chemically altering polymer chains to degrade over time, facilitating wound healing without the need for suture removal. Alternatively, natural materials like catgut, derived from sheep or goat intestines, provide absorbable options with

[a]*Laboratory for Innovations in Microengineering (LiME), Department of Mechanical Engineering, University of Victoria, Victoria, BC V8P 5C2, Canada.*
E-mail: makbari@uvic.ca
[b]*Center for Advanced Materials and Related Technologies (CAMTEC), University of Victoria, Victoria, BC V8W 2Y2, Canada*

† Electronic supplementary information (ESI) available. See DOI: https://doi.org/10.1039/d4nr01432d

variable absorption rates depending on processing methods.[13,14] Advanced techniques, such as electrospinning (ES), allow for precise control over suture diameter and composition, enabling the incorporation of bioactive agents or nanomaterials for enhanced wound healing properties.[15] ES is low-cost, reproducible, and allows simple fabrication and functionalization of sutures, and it can be done in different orientations of the apparatus, such as vertically or horizontally, to achieve different goals.[16,17]

Electrospinning is a robust technique for producing nanofiber coatings with controlled alignments on sutures by using rotating drum collectors, electrospun fiber pulling, and conductive patterned collectors.[18,19] The nanofibers in sutures can enhance wound healing and tissue regeneration[10] as well as help with the encapsulation and programmed release of drugs and other agents with antibacterial,[4] anti-inflammatory,[20–22] antioxidation, angiogenesis, cell migration for wound healing,[23] and more wound healing properties.[10,24] Furthermore, the alignment of nanofiber coatings promotes ordered cell growth along the matrix, creating tissue and organ function patterns.[25] With functionalization, sensing and actuation mechanisms can also be added to the suture to report on some situation in the wound, like sensors of bacteria[26] or to start releasing therapeutic agents.[27] Nevertheless, the process is currently constrained by its relatively low productivity, which poses challenges for scaling up suture production. Furthermore, the electrospinning process often faces the significant obstacle of low reproducibility in fabrication, necessitating extensive optimization experiments.[28–32]

Effective wound care is crucial in healthcare worldwide because of the common incidence and cost of wounds.[33] The optimal wound care process involves diagnosing the bacterial infection and administering appropriate therapeutic medications to enhance the outcome. Scientists are creating innovative techniques for diagnosing and treating infected and chronic wounds, and integrating diagnosis and therapy into a single approach, which is known as theranostics, has gained popularity as a more effective tool in recent years.[34] In more advanced forms of theranostic sutures, the drug release can be programmable instead of simply releasing the drug based on the degradation of the suture or, even better, in smart sutures or stimuli-responsive drug release when the sensing part can actuate the drug release to enhance the final wound healing outcome. Material functionalization methods with novel techniques for fabrication and functionalization have to be used to add those features to the suture.[35] Using sensors in smart dressings to release antibiotics for wound treatment has significantly advanced. The drugs can be released through external stimuli controlled by the user, or they can be programmed for slow release by designing drug entrapment or encapsulation.[36,37] However, in novel advanced approaches, triggering can involve internal stimuli like changes in the pH or temperature of the wound. This approach is more advantageous as it avoids the potential complications of incorporating a large device to be placed over the wound or adding them directly to the wound dressing.[38–40] Moreover, by using smart sutures instead of wound dressings, the wound is not only closed physically but various sensors and treatments for different types of wounds can also be integrated to enhance the capabilities of those sutures.[27,41,42]

In this work, we present a novel roll-to-roll coating approach for producing sutures with nanofiber coatings. Our method relies on direct electrospinning of polymeric biomaterials onto the suture material allowing for scalable production of functional sutures. We showcased the potential of the method to fabricate a smart suture able to release drugs based on temperature changes. There are a few reports of temperature-based drug release by introducing a stimuli-responsive suture, where release of the drug successfully promotes cell migration using a core–shell structured suture made of poly(vinyl alcohol) (PVA) grafted onto poly(*N*-isopropylacrylamide) (PNIPAm)[22] and a temperature-based drug-releasing suture for dexamethasone.[21]

2. Results & discussion

2.1. Characterization and mechanical testing results

The smart suture fabrication method is shown schematically in Fig. 1A, wherein a plain spool of thread or suture material mounted on a rotational bearing is connected to an empty receiving spool coupled to a clockwise rotating motor shaft. Suture tension between the spools is achieved when the motor is powered. The suture material is elevated using supports with through-hole guides and moves across an electrically grounded base collecting plate at a user-specified velocity. As the thread moves beneath the charged spinerette needle, electrospun nanofibers collect onto the surface of the thread, forming a nanofibrous coating. A syringe pump elevated above the base-collector plate controls the flow rate of a syringe containing liquid ES polymer solution. Electronic components, the user interface, and spooling motor are separated from the electrospinning device by an enclosure for spooling velocity, flow rate, and total run-time user interaction.

As shown in the cross-sectional SEM (scanning electron microscopy), images of coated sutures, single (Fig. 1B), and multiple (Fig. 1C) layers of different materials with distinct physical and chemical properties can be deposited sequentially. Numerous coating layers are achieved by passing the thread beneath the ES spinerette after the previous coating by reversing the spool placement. The surface ES coatings are shown to be uniform about the radius of the suture. During the process of ES, nanofibers are physically transferred to the surface of the suture. This manufacturing process allows for the fabrication of one-meter spools of smart sutures within minutes. Fig. 1D shows such a resulting spool of electrically conductive coated sutures.

The expectation of uniform suture coatings of different materials was tested, and successful layer deposition on smooth (monofilament) and rough (multifilament) surface materials was seen. This process was compatible with commercially available nylon upholstery threads and various suturing materials. ES PCL coatings, shown in white, were deposited onto five different commercial sutures, as shown in Fig. 1E,

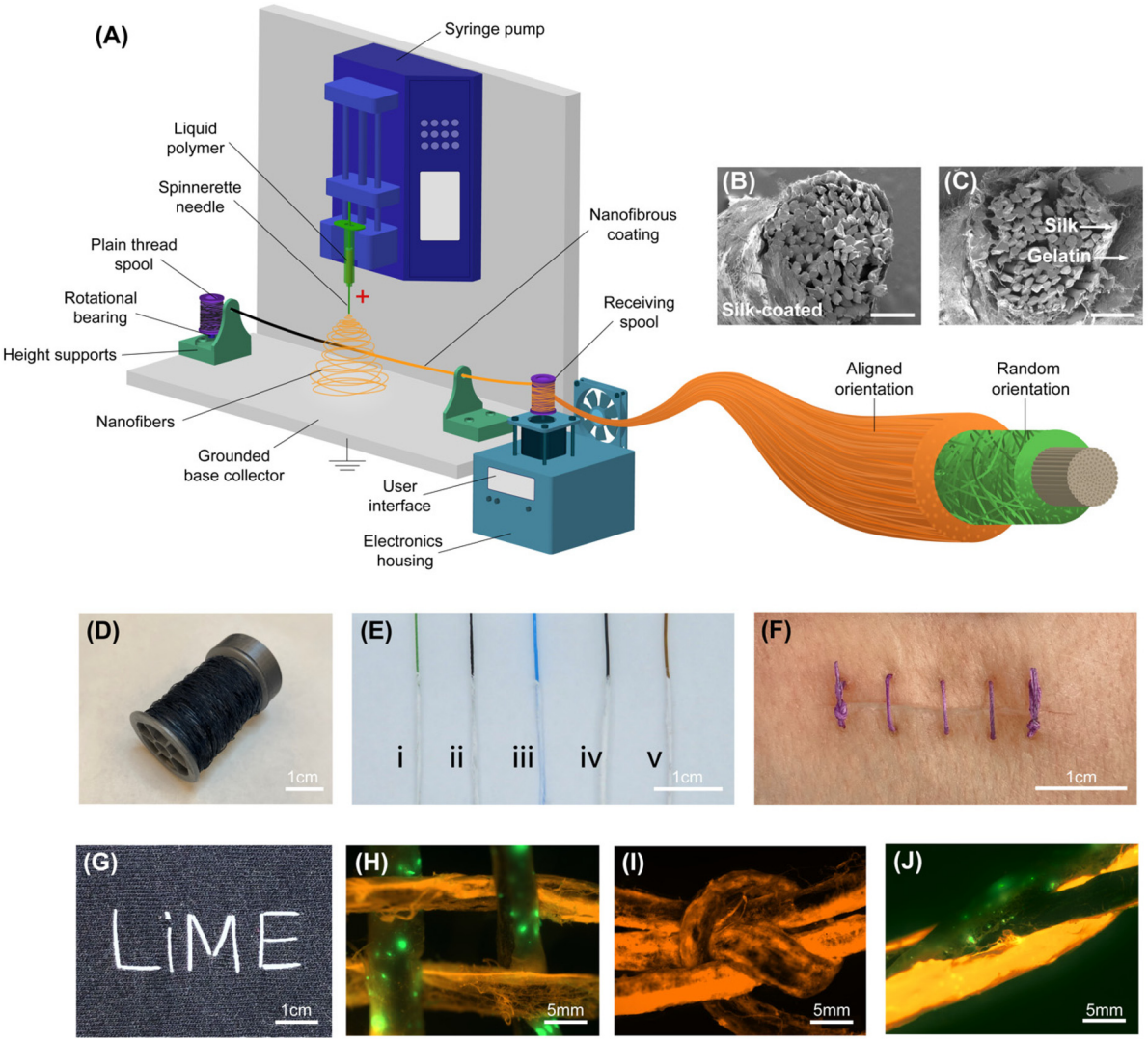

Fig. 1 Fabrication process and characterization of nanofiber-coated sutures. (A) Manufacturing setup for roll-to-roll coating of threads. SEM images of (B) single-layer and (C) multilayer coating prove uniform suture coating. (D) The manufacturing process allows 1 m spools of smart sutures to be prepared within 2 minutes. (E) The process is compatible with various suturing materials, including (i) nonabsorbable polyester, (ii) multifilament silk, (iii) monofilament polypropylene, (iv) monofilament nylon, and (v) absorbable chromic catgut. (F) As demonstrated in an *ex vivo* pig skin model, the coated sutures can close laceration wounds. The coating is strong and can withstand mechanical loads during various textile manipulations, including (G) braiding, (H) weaving, (I) knotting, and (J) embroidering.

labeled (i) to (v) for nonabsorbable suture materials of multifilament polyester, multifilament silk, monofilament polypropylene (Prolene), monofilament nylon (Ethilon), and absorbable chromic catgut, respectively (Fig. 1E). Delamination of the ES coatings from the suture surfaces did not occur when sutures were drawn through biological tissues (mounted on a 25 mm reverse cutting needle). In a wound model where a laceration was created *via* scalpel in 4 mm-thick *ex vivo* pig skin, the tissue edges were approximated together with coated sutures (shown in pink in Fig. 1F). Coated threads were then embroidered into cotton fabric using a conventional sewing needle, further demonstrating the sturdiness of the ES coating (shown in white, Fig. 1G). The ES coating demonstrated strength and the ability to withstand mechanical loads during various textile manipulations. The versatility of these constructs is demonstrated with gelatin-coated sutures (green, dyed with FITC-dextran) combined with silk fibroin-coated sutures (orange, dyed with rhodamine) and plain sutures (non-fluorescent) in braided (Fig. 1H), woven (Fig. 1I), and slip knot-knitted (Fig. 1H) applications.

2.2. Results of testing different biomaterials for suture coating

Three materials were chosen to represent the flexibility of the developed fabrication method: gelatin, PCL (polycaprolactone), and silk fibroin. PCL is a biodegradable synthetic polymer with a history of regular use in medical applications.[26] Slow biodegradability characteristics and easy combination of PCL with other polymers for forming composites and co-polymers make it a desirable material for scaffolds used in tissue engineering, surgical sutures, and micro- and nano-drug deliv-

ery applications.[43] PCL coatings were achieved with 15 w/w% of PCL in DCM (dichloromethane) and methanol organic solvents,[44] with a flow rate of 0.1 mL h^{-1}, applied voltage of 14 kV, and varied spooling velocities and needle-thread distances. Silk fibroin is a natural high molecular weight protein polymer produced by the silkworm species *Bombyx mori* and used extensively as a polymeric biomaterial for drug delivery.[45]

Silk fibroin also exhibits beneficial properties such as high biocompatibility, biodegradability, aqueous processing, and the ability to form crystalline polymer matrices. Researchers found that silk fibroin with a concentration of 13 w/w% in formic acid demonstrated being electro-spinnable at room temperature;[46] suture coatings with this liquid polymer were achieved using a flow rate of 0.07 mL h^{-1}, applied voltage of 16 kV, spooling velocity of 3 mm s^{-1}, and needle-thread distance of 2 cm.

Gelatin is a highly biocompatible, bioactive, and hydrophilic biopolymer, properties that make it a promising scaffolding material for recapitulating the ECM. This natural polymer's high biocompatibility and bioactivity result from its specific amino acid sequences, which are preferable sites for cell interactions. Preparing this material using ES methods results in a structure with a smooth surface and a large surface area-to-volume ratio. Researchers Ki *et al.* electrospun 13 w/w% gelatin from porcine skin dissolved in formic acid to form ultrafine fibers; ES coatings fabricated using this method were further achieved utilizing a flow rate of 0.07 mL h^{-1}, applied voltage of 16 kV, spooling velocity of 3 mm s^{-1}, and needle-thread distance of 2 cm.

To demonstrate the efficacy of the chosen ES parameters with these polymers and the structural features of the fabricated electrospun substrates, SEM images of the ES fiber morphologies were taken. In Fig. 2A, SEM images of (i) gelatin, (ii) PCL, and (iii) silk fibroin show nanofibers deposited onto curved thread surfaces. The images show differences in both fiber diameter and pore size of the resulting ES coating. The average diameters of the fibers in the nanofibrous hydrogel of PCL, gelatin, and silk fibroin were 3.56 ± 2.12 μm, 1.43 ± 0.24 μm, and 1.38 ± 0.37 μm, respectively. The resulting fiber morphology of the three polymer coatings on sutures was found to be comparable to that of ES mats formed on flat base collectors.[47]

The characteristics of the PCL ES coating were found to be dependent on the individual factors of the electrospinning setup. Spooling velocity and the displacement between the spinnerette needle tip and the surface of the thread affect the thickness of the coating layer (parameters shown in the schematic of Fig. 2B). Similarly, under stationary conditions, the duration of electrospinning linearly increases the coating thickness (ESI, Fig. S1†). The flow rate was optimized and kept constant for layer thickness tests of each material, as increased flow rates result in increased fiber diameter, volume, and initial radius of the electrospinning fiber.[48]

Layer thickness was measured from the measurable diameters of sutures in microscope images before and after coating. At a height of 6 cm, the layer thickness was found to decrease with increasing spooling speed (Fig. 2C). Layer thickness was found to be 211.52 ± 49.43 μm under stationary conditions, while 3.50 ± 3.11 μm at 17 mm s^{-1}. The displacement between the needle and the thread surface was varied by replacing the guiding height support blocks shown in Fig. 1A. The layer thickness increases when the suture–needle displacement is incrementally increased (constant spooling velocity of 10 mm s^{-1}), possibly due to electric field strength and nanofiber flight duration. Increasing the distance between the needle and the collector (spooling thread) has been shown to reduce the ES fiber diameter due to the greater stretching distance.[49]

The spooling velocity changes the orientation of the nanofibers from random (Fig. 2E) to aligned (Fig. 2F) on the suture surface. In the rotating drum ES method, electrospun fiber deposition onto a moving collector thread was hypothesized to align in uniaxially aligned arrays. The angle of deposited electrospun fibers on the surface of the thread was measured with respect to the direction of the length of the thread and measured from SEM images taken of the surface coating. At lower velocities (1–10 mm s^{-1}), a high standard deviation in fiber orientation indicated the random and unaligned nature of the deposited fibers. At higher velocities (12.5–17.5 mm s^{-1}), the fiber angle approached zero, and the standard deviation decreased, demonstrating the alignment of fibers along the length of the thread (ESI, Fig. S2†). The frequency distributions of the deposited fiber orientation for 1 mm s^{-1} and 17.5 mm s^{-1} spooling velocities are shown in Fig. 2E and F, respectively. At 17.5 mm s^{-1}, a Gaussian distribution (R = 0.9655) was seen, compared to a random distribution at 1 mm s^{-1} spooling velocity. This indicates the fiber orientation is random with respect to the direction of the thread at low spooling velocities.

2.3. Results of thermo-responsive coating and drug release

Among electrically conductive materials, poly(3,4-ethylenedioxythiophene):poly(styrene sulfonate) (PEDOT:PSS) is a good candidate for biosensing applications and has been extensively used for amperometric,[50,51] impedimetric,[52,53] and voltammetric biosensors.[54,55] PEDOT:PSS has exceptional optical transparency in the visible light range, high electrical conductivity, high work function, and favorable physical and chemical photo- and electrical stability in air. The suture coatings were achieved by combining an aqueous dispersion of PEDOT:PSS 1 : 10 with PEO (polyethylene oxide) as an electrospinning agent, dissolved in DMF (dimethylformamide) organic solvent.[56] The poor rheological properties of PEDOT:PSS require using a carrier polymer (*i.e.*, PEO) to process it. A polymer flow rate of 0.07 mL h^{-1}, applied voltage of 16 kV, thread-needle displacement of 3 cm, and spooling speed of 3 mm s^{-1} were used to fabricate the conductive sutures. Fig. 3A depicts the randomly oriented nanofibrous conductive coatings on the core suture. As a proof-of-principle, a 2 cm-long conductive-coated thread was used as a wire between a power source (5 V) and ground, as seen in Fig. 3B. The thread successfully acted as an electrically conductive wire, allowing an in-series LED (light emitting diode) to be illuminated with

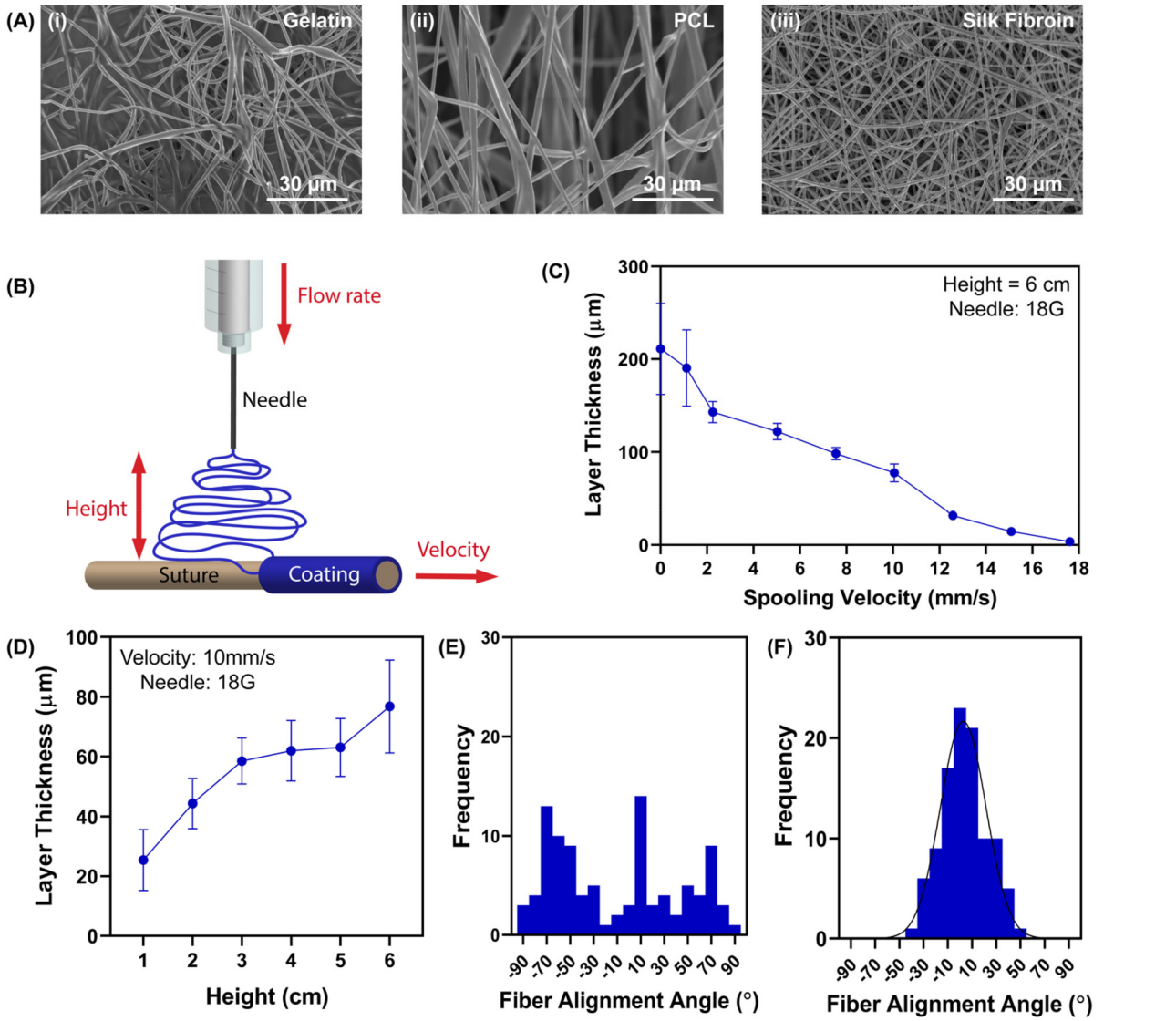

Fig. 2 Testing the developed method with different biomaterials for the coating. (A) SEM images of (i) gelatin-, (ii) PCL-, and (iii) silk fibroin-coated threads confirm a nanoporous coating on the core sutures (scale bars: 30 μm). (B) The thickness of the coated layer depends on the spooling velocity and needle height (suture–needle distance). (C) The thickness of the coated layer decreases with spooling velocity. (D) The layer thickness increases with suture–needle distance. The spooling velocity changes the orientation of the nanofibers from (E) random to (F) aligned orientation in the coated layer.

completion of the circuit. The mean resistance of the conductive threads was measured to be 55 ± 23 kΩ cm^{-1} at ambient temperature (21 °C). The average conductive electrospun layer thickness was 68.11 ± 7.19 μm.

The extended response of conductive electrospun-coated threads at a physiologically relevant temperature was characterized by relative humidity (RH) of 30% (Fig. 3C). Over 30 min, the resistive response of the thread was measured and appeared approximately constant; the measured resistance varied by only 5%. This preliminary study indicates that the resistance of the threads does not change considerably under constant temperature conditions. PEDOT:PSS/PEO electrospun-coated threads demonstrated an inverse change in resistance with applied heat, as shown in Fig. 3D. At 30% RH, the electrical resistance of the thread was measured under dynamically increasing temperature (total change of 30 °C). The resistance of the coated suture showed a sensitive response (70% resistance change) over the 75 minutes of the test duration. An application area for these threads is in wound beds or deep tissue environments, where the increased localized wound temperature is an initial diagnostic sign of wound infection.[57]

Conductive threads can also be used to trigger drug release if combined with thermo-responsive PNIPAm coatings. PNIPAm demonstrates thermo-responsive behavior at 32 °C in aqueous solutions, undergoing reversible phase transition in response to environmental temperature changes. Below 32 °C, PNIPAm is hydrophilic; upon increasing the temperature, PNIPAm becomes hydrophobic, and the rapid dehydration of

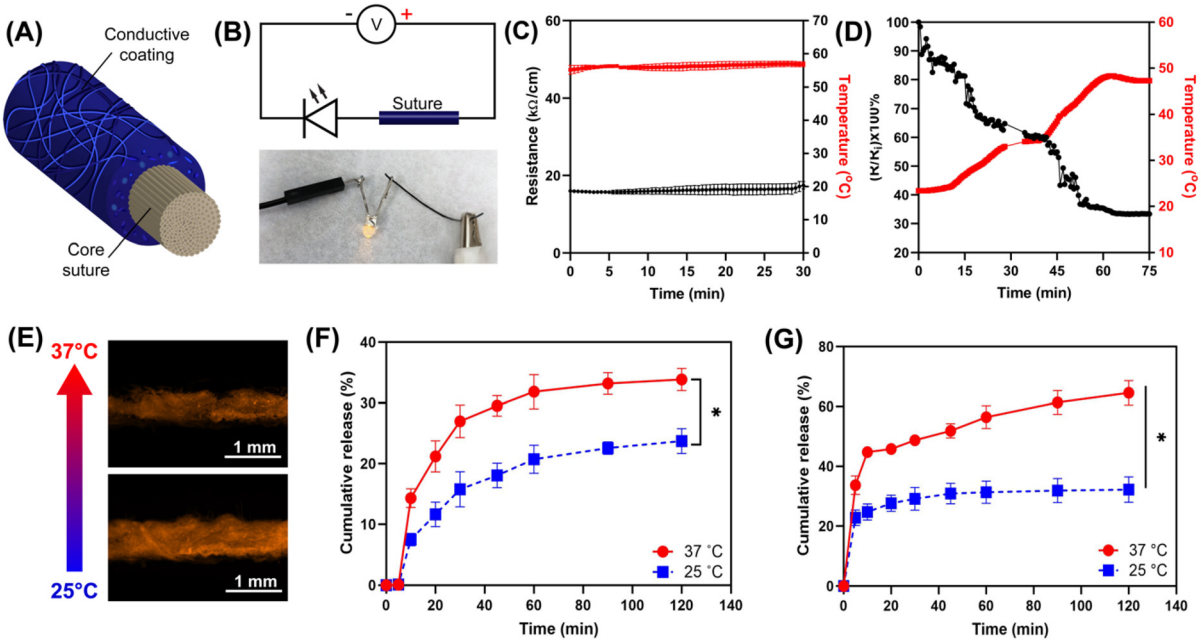

Fig. 3 Testing for conductivity and triggered-release drug delivery and temperature sensing. (A) Electrospinning of PEDOT:PSS on a core suture renders it electrically conductive, where (B) it acts to complete a circuit to light an LED lamp. (C) The conductive layer is stable under constant temperature conditions. (D) The resistance of the sutures varies with temperature, which suggests its use for temperature sensing. (E) Conductive threads can be used for the triggered release of drugs when they are combined with thermo-responsive PNIPAm coatings. Temperature-dependent release (%) of two model drugs, including (F) small molecules (rhodamine B, 470 Da) and (G) large molecules (FITC-dextran, 20 kDa), demonstrate the ability of triggered-release of drugs using smart sutures.

the polymer network results in the release of encapsulated drug components. PNIPAm–PCL ES coatings were achieved with a 1 : 4 ratio of the solid polymers dissolved in DCM/methanol solvents, 15 kV applied voltage, spooling velocity 8 mm s^{-1}, 0.05 mL h^{-1} flow rate, and thread-needle displacement of 8 cm.[58] PNIPAm and PCL blended polymers have been shown to generate electrospun fibers with high cell viability and cell alignment that can suppress the release of loaded drugs at higher temperatures.[59] Thus, the fluorescent images shown in Fig. 3E of rhodamine B-loaded PNIPAm–PCL sutures show the shrinking response of the outer coating upon heating at about 32 °C.

Similarly, two dyes (FITC-dextran and rhodamine B) as drug models were added to PNIPAm–PCL polymer solutions before ES and used to fabricate single-coating sutures. The fluorescence from the release of dyes into PECF (pseudo extracellular fluid)[60] was measured *via* a plate reader using experimentally determined calibration curves of fluorescence intensity (ESI, Fig. S3†). Fig. 3F shows the percentage of cumulative release of small drug model rhodamine and (Fig. 3G) large drug model FITC-dextran from PCL/PNIPAm-coated threads at 25 and 37 °C over a 2 h period. The cumulative release of FITC-dextran reached 64.55 ± 4.08% and 32.23 ± 4.28% for 25 and 37 °C, respectively. The cumulative release of rhodamine B was lower and reached 23.5 ± 1.52% and 34.3 ± 2.01% for 25 and 37 °C, respectively.

The release of both drug models was significantly different for 25 and 37 °C, which shows the temperature-responsive nature of the applied suture coatings. Due to the heat, this substantial difference can be used for smart stimuli-responsive release of both small and large molecules of therapeutic agents. While both release profiles show an initial burst, this is followed by a gradual release; the burst release of FITC-dextran was observed to occur fully within the first 5 min of testing. Hydrophilic small molecule drugs (*e.g.*, rhodamine B) have high aqueous solubility and are incompatible with insoluble polymers, which makes their long-term release challenging.[61] Therefore, the lower cumulative release of rhodamine may be due to the solute–polymer interactions and incompatible solubility parameters of rhodamine (27.4 MPa) and PCL/PNIPAm (18.25 MPa and 21.9 MPa, respectively). The burst release of drugs from polymeric nanocarriers has been identified as a significant limitation in achieving controlled drug delivery.[45] To prevent the initial burst releases seen in Fig. 3F and G, drugs and bioactive factors may instead be loaded into the core of multi-axial nanofibers obtained by coaxial or triaxial electrospinning.[59]

2.4. Cell and biocompatibility results

High cell-viability requirements exist for sutures as they make direct or indirect contact with cells and tissues during wound approximation and when used as a means of fixation for anchoring devices and implants within the body. The viability of HaCaT cells attached to the sutures was used to determine the biocompatibility of three electrospun polymer (gelatin, silk fibroin, and PCL)-coated suture types. This cell line was chosen as keratinocytes play an essential role in wound

healing and re-epithelialization.[62] The suture type viability was measured by the percentage of live HaCaT cells on days 3 and 7. Fig. 4A shows gated dot plots of the live and dead populations for gelatin and silk fibroin-coated sutures from stained cells, excluding debris from the plots. Flow cytometry results for gelatin and silk fibroin show more than 90% cell viability for cells exposed to gelatin and silk fibroin smart sutures after detachment at days 3 and 7 (Fig. 4A).

The quantitative analysis of HaCaT cell viability showed that the detached cells are highly viable when exposed to silk fibroin-, gelatin-, and PCL-coated sutures for 7 days (Fig. 4B). The observed percentage of dead cells relative to the number of living cells decreased for the three sample groups between days 3 and 7. The numerical live/dead results show that the number of live cells significantly increased between days 3 and 7 for the gelatin, silk fibroin, and PCL sample types. Additionally, gelatin and silk fibroin-coated samples demonstrated higher viability (94.7 ± 0.35% and 93.47 ± 0.30%, respectively) than PCL (88.5 ± 1.99%) at day 7. The increased viability and biocompatibility of the gelatin and silk fibroin polymer-coated sutures point towards their potential benefits as scaffolding materials for 3D tissue-engineered scaffolds assembled using textile-based methods. The relatively high viability for all three sample types subsequently shows that the proposed electrospinning fabrication and crosslinking processes do not negatively impact biocompatibility or the ES-coated sutures or result in the formation of cytotoxic residues.

HaCaT cells were similarly used to quantitatively study cell attachment and proliferation on the three electrospun polymer types. Cell adherence to a scaffold substrate is a fundamental

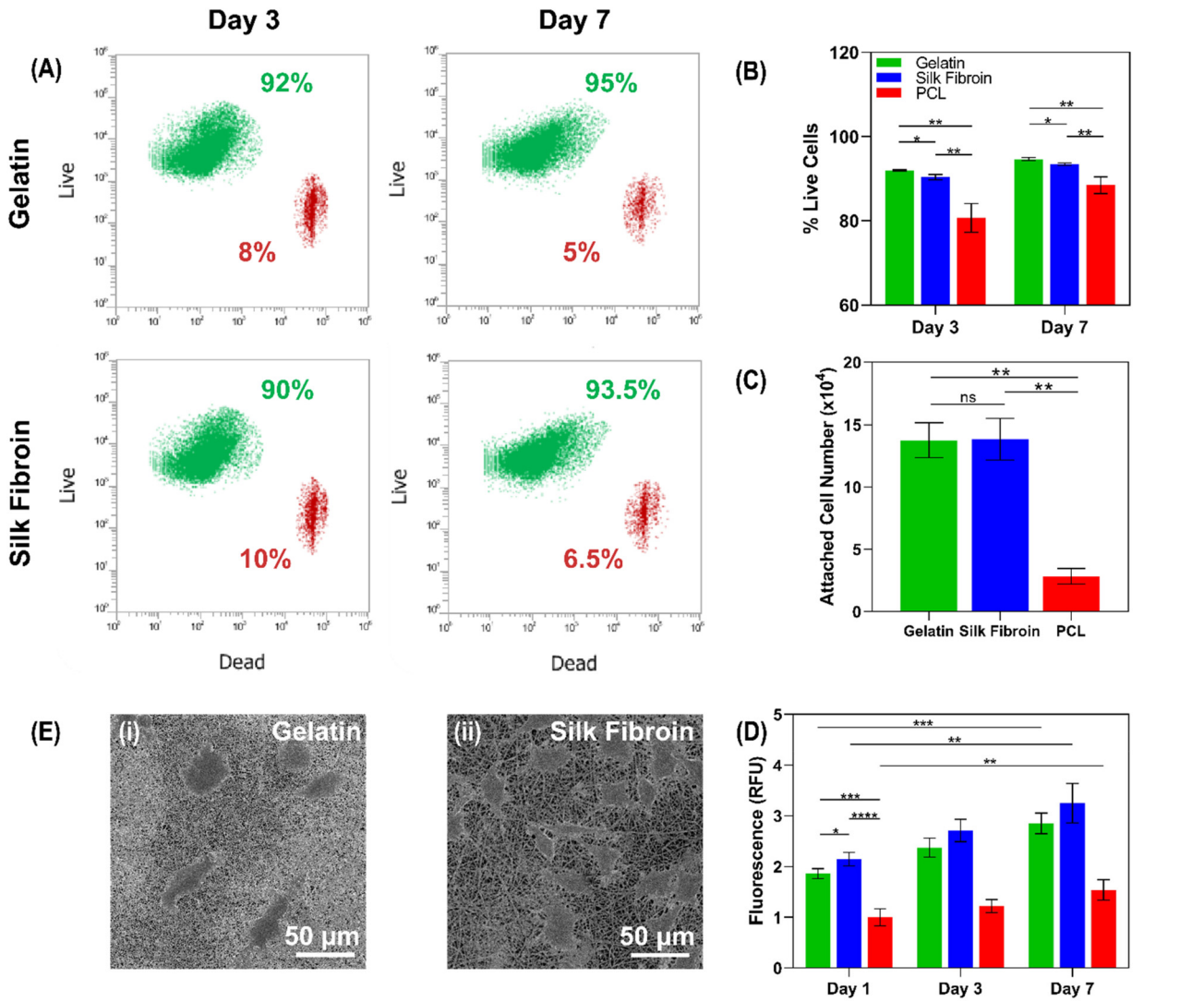

Fig. 4 Biocompatibility and cell attachment studies for the coated sutures. (A) Flow cytometry results for gelatin and silk fibroin results show more than 90% cell viability for cells exposed to gelatin and silk fibroin smart sutures. (B) Quantitative analysis of cell viability shows that the cells are highly viable when exposed to silk fibroin-, gelatin-, and PCL-coated sutures for 7 days. (C) Cell attachment on PCL is significantly lower than that on silk fibroin- and gelatin-coated sutures. (D) Proliferation on PCL coatings is significantly lower than that on silk fibroin- and gelatin-coated sutures. (E) SEM images demonstrate cell attachment and spreading on the latter sutures (scale bars: 50 µm).

preliminary step for further cell–substrate interactions by promoting cell proliferation, migration, and differentiation. Multiple research groups have demonstrated high rates of cell proliferation on silk fibroin scaffolds.[63] While gelatin nanofibrous mats that are crosslinked with glutaraldehyde vapor become more water-resistant, the nanofibrous structure of electrospun gelatin has been found to enhance cell adhesion and proliferation, and the RGD (arginine–glycine–aspartic acid) sequences of collagen make it highly effective for cell adhesion.[64] Other than the nonspecific binding of cells to electrospun PCL samples, PCL is intrinsically hydrophobic.[65] It lacks functional groups such as RGD-motif-containing cell-attachment peptides that provide specific binding sites for cells.[66,67]

After cultures of 10^6 HaCaT cells on coated suture samples, the measurement of cell attachment on the surface of gelatin- and silk fibroin-coated sutures was found to be insignificant (Fig. 4C). The cell attachment on PCL was significantly lower than that on silk fibroin- and gelatin-coated sutures ($^{**}p < 0.001$, $^{**}p < 0.001$, respectively). While cell adherence to implanted sutures is fundamental in the promotion of cell proliferation, migration, and differentiation, the low cell attachment of PCL-coated sutures may have benefits for applications where low cell adhesion is preferable; for example, non-absorbable sutures that require removal after wound healing should have low cell adhesion properties to improve the ease of removal, reduce patient pain, and reduce injuries to adjacent tissues. Furthermore, Badami *et al.* postulated that the differences in electrospun fiber diameter and the resulting surface topography between ES polymers (*e.g.*, silk fibroin, gelatin, and PCL) may cause significant effects on cell morphology and cell proliferation.[68]

Cellular proliferation was calculated by measuring the metabolic activity of cells seeded on coated sutures at days 1, 3, and 7 and are reported in relative fluorescent units, as seen in Fig. 4D. Proliferation on gelatin, silk fibroin, and PCL suture samples increased significantly between days 1 and 7 ($^{***}p < 0.0001$, $^{**}p < 0.01$, $^{**}p < 0.01$, respectively). After 24 hours of culture, cell proliferation was lowest in PCL-coated sutures. Gelatin- and silk fibroin-coated samples showed less significantly different cell proliferation, with silk fibroin having the highest proliferation of the three sample types.

Fibroblast cells, which play a central role in wound healing and are among the most common cells of connective tissues in humans, were seeded on the three polymer-coated sutures to determine the differences in attached cell morphology and spreading on randomly aligned ES nanofibers. Fibroblasts were chosen due to the ease of culture and their presence in tissue injuries such as partial- and full-thickness lacerations. The morphology of fixed fibroblasts after 24 hours of culture is shown in SEM images of (i) gelatin- and (ii) silk fibroin-coated sutures (Fig. 4E). The fibroblast cells growing on gelatin and silk-fibroin nanofibers have dispersed patterns and exhibit more isotropic morphologies on the randomly oriented fibers, with clear borders between the cells and the nanofibers. These morphologies may be due to the hydrophilic nature and high cell adhesion properties of the two natural polymers.[69,70]

Our recently developed electrospinning fabrication technique is a notable breakthrough in manufacturing theranostic sutures. This method utilizes a roll-to-roll process to improve the efficiency and cost-effectiveness of suture manufacturing. In the past, the production of sutures has faced operational challenges due to expense, lengthy time commitments, and multiple complex steps.[23,27,41] Our technique addresses these issues by significantly reducing time consumption and increasing ease of use while achieving higher throughput. These enhancements are accomplished without sacrificing cost-efficiency, which is especially important considering the financial limitations commonly found in medical production. In addition, our technique enables the ongoing fabrication of sutures that possess both flexibility and substantial biological characteristics while maintaining mechanical features for higher stability and a more controlled rate of drug release compared to previous studies with fast and high burst release within the first few hours.[39,71] Our technique enables the precise modification of the coating layer's thickness and the alignment of the nanofibers, allowing for the precise adjustment of the physical and chemical properties of the suture in very easy steps, whereas previous studies mostly consist of long fabrication times (even up to 72 hours).[72] This ability is of utmost importance for wound closure and infection control applications, particularly through advanced drug delivery systems. The sutures created using this technique can be seamlessly integrated into various medical applications, thus extending their usefulness beyond conventional purposes.

The innovation of our methodology lies in the precise modification of the microstructural properties of the suture material, which facilitated more controlled drug release rates. While some configurations exhibited a markedly slow release, with up to 90% of the drug being released over 200 hours at 37 °C,[22] others demonstrated that 80% of the drug was released within the first 72 hours.[73] In contrast, some models showed minimal release, with less than 16% released over a period of 7 days, and some configurations exhibited exceptionally prolonged release durations.[4] In addition, the ability to adjust the thickness and alignment of the material, along with its natural flexibility, makes it simple to manipulate and apply the coated threads. Flexibility is essential when dealing with diverse biomedical settings, such as direct contact with the skin and incorporation into wound dressings. Finally, our approach was validated across both small and large molecular entities, in contrast to prior studies, which were predominantly concentrated on single-model drugs.[2,3,20,21,74]

3. Conclusion and future perspectives

Clinical sutures are primarily used for the physical approximation of tissues. However, developing new suture materials with surface modifications toward improved healing outcomes plays upon the inherent versatility of thread technologies. Similarly, ES has been extensively studied in biomedical and

tissue engineering, given its compatibility with synthetic and naturally biocompatible polymers and its capacity for loading bioactive and functional additives into the resulting nanofibrous constructs. A novel method was proposed, which involves continuously fabricating single-layer and multi-layer smart sutures through functionalization using ES coatings of a wide range of polymers with distinct biological characteristics. Various parameters in the methodology, such as ES run time, spooling velocity, and displacement between the spinerette needle and the thread, can be controlled by the user to suit the given application, providing adaptability of coating layer thickness and ES nanofiber alignment with respect to the direction of the thread. The flexibility of nanofibrous-coated threads offered easy manipulation with materials such as biological tissues and fabric while also facilitating the combination of coated sutures using traditional textile methods. Smart multifunctional sutures and threads were developed and applied in biosensor miniaturization, targeted drug delivery systems, and tissue engineering.

The primary objective of future research should be to enhance the biocompatibility and functional performance of these sutures coated with nanofibers in clinical settings. This can be accomplished by integrating sophisticated bioactive substances such as stem cells, immune cells, growth factors, or multifunctional bioactive agents. These enhancements can accelerate the healing process and enhance the therapeutic effectiveness of sutures designed for wounds or infections. Integrating sensors into sutures, coupled with the utilization of real-time data capture technologies, has the potential to revolutionize postoperative care. This would enable healthcare providers to promptly receive feedback and make real-time adjustments based on the conditions of the wound. Pioneering the advancement of sophisticated control systems to regulate the kinetics of drug release, as well as conducting extensive investigations into the compatibility with living organisms and the breakdown patterns within them, is crucial for accurately synchronizing drug administration with the various stages of healing. These advancements could lead to the creation of advanced smart sutures beyond simply assisting in tissue healing and integration. Researchers could also establish smart sutures as an integral part of modern surgical procedures and introduce new approaches to personalized medical care. Future research should prioritize conducting comprehensive *in vivo* studies to further evaluate the biocompatibility and stability of these sutures coated with nanofibers. It is crucial to conduct clinical safety evaluations involving cytotoxicity studies and other biological experiments using animal models to assess the long-term behavior of the suture. The clinical feasibility and safety of the sutures, as well as the lack of negative reactions during their intended period of use, rely on these investigations. By incorporating these studies, the suitability of the sutures for widespread medical use will be confirmed. This aligns with efforts to enhance their therapeutic efficacy and intelligent features, allowing for real-time monitoring and adaptive responses to healing conditions.

4. Materials and methods

4.1. Threads and sutures

3-0 Multifilament polyester suture (Ethicon Inc., USA), multifilament silk (Ethicon Inc., USA), 3-0 monofilament polypropylene (Prolene, Ethicon Inc., USA), 2-0 monofilament nylon (Ethilon, Ethicon Inc., USA), and 3-0 chromic absorbable surgical catgut sutures (G122H, Ethicon Inc., USA) were tested for their applicability with ES coatings. Quantitative experiments were performed on multifilament 100% nylon upholstery thread (Coats & Clark Inc., USA).

4.2. ES fabrication setup

A programmable syringe pump (New Era Pump Systems, USA) was positioned above the base-collector on a platform. ES solutions were loaded into syringes, and blunted 18G needles were attached. The needle and base-collector were attached to the positive and negative terminals of a high-voltage power supply (Gamma High Voltage Research, USA). The syringe was held at a constant distance from the base-collecting plate. A custom spooling system moved the thread horizontally beneath the syringe, above the collector plate at a defined velocity. The spooling setup consisted of a stepper motor (SparkFun Electronics, USA) controlled by an Arduino Uno (Arduino, USA) and Arduino Motor Shield Rev3 (Arduino, USA). At the same time, the stationary thread was moved horizontally, within a movable range of 1–6 cm (thread displacement) relative to the spinnerette needle. The user interface was an LCD (liquid crystal display) screen (HD44780, Adafruit, USA) with a physical push-button makeup, allowing the user to set the spooling velocity and total run duration. All ES experiments were performed at room temperature (21 °C) and relative environmental humidity.

4.3. Material preparation for threads coating

4.3.1. PCL. 15 w/w% PCL (MW 45 000, Sigma Aldrich, USA) was dissolved for ES in a 4 : 1 ratio of dichloromethane (DCM) (CH_2Cl_2, Sigma Aldrich, USA) and methanol (Fisher Chemical, USA). The solution was kept under constant agitation at room temperature for 2 h until the solution became homogeneous.

4.3.2. Gelatin. 13 w/w% gelatin (~300 g Bloom, Type A, Sigma Aldrich, USA) was dissolved in formic acid (Sigma Aldrich, Saint Louis, USA) and kept under constant agitation at room temperature for 8 h until the solution became homogeneous. The nanofibrous-coated threads were crosslinked in the glutaraldehyde vapor (Grade 1, 25% solution in H_2O, Sigma Aldrich, USA). Briefly, 3 mL of glutaraldehyde solution and 100 μL of HCl (37%, Sigma Aldrich, USA) were added to 20 mL of dH_2O (distilled water) in a 10 cm Petri dish. Gelatin-coated threads were suspended above the Petri dish within a sealed vacuum chamber for 6 h until a visible color change from white to yellow occurred. A final washing step to remove the glutaraldehyde residues was performed. Threads were rinsed three times in 1% glycine (NH_2CH_2COOH, Sigma Aldrich, USA) in dH_2O for 10 min, followed by 10 min in dH_2O.[50]

4.3.3. Silk fibroin. Silk cocoons from *Bombyx mori* were obtained from the Iranian Silkworm Research Center and boiled in 0.02 M aqueous sodium carbonate (Na_2CO_3; 106392, Merck, Germany) solution for 1 h to remove sericin, washed with dH_2O and dried at 37 °C overnight. The degummed silk was then dissolved in 9.3 M lithium bromide (LiBr; 746479, Sigma-Aldrich, Saint Louis, USA) at 60 °C for 4 h, then dialyzed in a cellulose dialysis tube (12 kDa, Sigma Aldrich, Saint Louis, USA) against deionized water (diH_2O) for 72 h. The silk solution was then lyophilized (MC4L, UNICRYO, Freeze-dryer, Germany) into prepared sponge,[75,76] which was dissolved at 13 w/w% in formic acid under constant agitation for 8 h. Electrospun silk fibroin was crosslinked by immersion in 70% ethanol (Sigma Aldrich, USA) for 10 min.

4.4. Preparation of drug-loaded threads

Fluorescein isothiocyanate-dextran (FITC-dextran, Sigma Aldrich, USA) and small molecule rhodamine B (Sigma Aldrich, USA) were used as large molecule and small molecule fluorescent drug models, respectively. They were added to 100 μL of dH_2O and vortexed to dissolve completely, and then the aqueous solution was added to silk fibroin ES solution at a concentration of 1 mg mL^{-1} fluorescent drug models and vortexed to mix thoroughly in a dimmed light environment.

4.5. Preparation of temperature-responsive threads

0.134 g of PEO (polyethylene oxide, Sigma Aldrich, USA) was dissolved in 0.345 mL of DMF, and 2.56 g of PEDOT:PSS PH1000 aqueous solution (poly(3,4-ethylenedioxythiophene): polystyrene sulfonate, Ossila, UK) was combined at room temperature, under constant stirring for 24 h. Electrical resistance was measured by following a two-point probe method using a digital multimeter (Fluke 87 True RMS Multimeter, Fluke, Canada). In addition, 10 w/v% PCL was dissolved in a 4 : 1 ratio of DCM and methanol. 10 w/v% PNIPAm (MW = 300 000 Da) was dissolved in a 4 : 1 ratio of DCM and methanol. The solutions were then combined and stirred until homogeneous at room temperature (1 h). FITC-dextran, rhodamine, and doxycycline hydrochloride (MW = 444 Da, Sigma Aldrich, USA) were added separately to 100 μL of dH_2O and vortexed to dissolve. The fluorescent drug models were added to ES solutions at a concentration of 1 mg mL^{-1}. Coated samples were washed in dH_2O for 30 min at 200 rpm on a plate shaker (Titer Plate Shaker 120V, Thermo Scientific, USA) to remove all excess unattached drugs.

4.6. Characterization with SEM imaging

SEM images were acquired by using a Hitachi electron microscope (Hitachi S4800, Tokyo, Japan) with 1.0 kV voltage to determine the structural features of the fabricated electrospun substrates. Samples were mounted on aluminum stubs using double-sided tape and then coated with gold–palladium *via* hummer sputter (Hummer VI Sputter Coater, Anatech USA, Hayward, CA, USA).

4.7. Cell viability of threads

Human primary keratinocytes (HaCaT; Addexbio, USA, catalog no. T0020001) were cultured in Dulbecco's modified Eagle's medium (DMEM; Gibco, Thermo Fisher Scientific, USA) supplemented with 10% fetal bovine serum (Gibco, Thermo Fisher Scientific, USA) and 1% penicillin–streptomycin (Gibco, Thermo Fisher Scientific, USA). The cells were cultured in cell culture flasks (T 75, VWR, USA) until they reached 80–90% confluency and were detached using trypsin–EDTA (0.5%, Gibco, Thermo Fisher Scientific, USA) before seeding on the electrospun-coated threads. Coated-thread samples were placed in non-adherent PDMS-coated wells, to which 50 μL of cell suspension containing 1×10^6 cells was added, with 950 μL of cell media subsequently added after 2 h. The viability of cells grown on the coated threads after 3 and 7 days was determined by a flow cytometer (Attune NxT, Thermo Fisher Scientific, USA). To this end, cells were initially detached from the threads described above and stained using a live/dead viability kit (Invitrogen, Thermo Fisher Scientific, USA) according to the protocol provided by the supplier.

4.8. Cell attachment of threads

Three samples (1 cm long) were placed in each well of a 24-well plate coated with non-adherent agarose. Cell seeding was carried out by adding 50 mL of a cell suspension that contained 1×10^6 HaCaT cells in culture media. After two hours of incubation, 950 μL of culture media was added to a final volume of 1 mL. 24 h after cell seeding, the threads were gently washed with culture media twice to remove non-adhered cells, and the cells were treated with 250 μL of trypsin–EDTA (0.25%) for 15 min to detach cells from the surface of the threads. 500 μL of cell media was then added to deactivate the trypsin–EDTA, followed by centrifugation of the supernatant at 300*g* to make a cell pellet. The supernatant was then removed, and the cell pellet was resuspended in 1 mL of cell culture media. Finally, 10 μL of cell suspension was stained with Trypan blue (Gibco, Thermo Fisher Scientific, USA), and the number of cells was counted using a hemocytometer.

4.9. Cell proliferation rate on threads

The proliferation rate of HaCaT cells on gelatin-, silk fibroin-, and PCL-coated samples after 1, 3, and 7 days was calculated by measuring the metabolic activity of cells at these time points. Cells were seeded on three 1 cm-long threads per well, as described previously. At specific time points, the culture solution replaced the PrestoBlue media and was incubated for 30 min. 100 μL of supernatant was removed from each well and plated in a 96-well plate. A microplate reader measured fluorescence intensity at excitation (560 nm) and emission wavelengths (590 nm). The relative proliferation rate was calculated by normalizing the measured intensity under each of these conditions with respect to the conditions with the lowest intensity.

4.10. Statistical analysis

Results were analyzed using GraphPad Prism Version 8 (GraphPad Software, CA, USA). Statistical significance was analyzed using an unpaired parametric *t*-test for two independent samples, not assuming equal deviations. Experimental results were obtained from biological replicates ($n = 3$). The mean and standard deviation were reported. *P*-value reporting is as follows: $*p < 0.05$, $**p < 0.01$, $***p < 0.001$, $****p < 0.0001$.

Author contributions

T. W. designed and analyzed the experiments, Z. H. performed bacterial and animal experiments, S. M. H. D. performed cell experiments, S. H. performed SEM imaging, S. S. performed SEM imaging, M. A. and T. W. drafted and edited the manuscript, and M. A. conceived the presented idea. All authors contributed to the final manuscript.

Data availability

Data will be made available upon request from authors. The data supporting this article have been included as part of the ESI.†

Conflicts of interest

There are no conflicts of interest to report.

Acknowledgements

The authors acknowledge the funding received from the Canadian Institutes for Health Research (CIHR), Canadian Foundation for Innovation (CFI), and BC Knowledge Development Fund (BCKDF).

References

1 H. Kim, B. H. Kim, B. K. Huh, Y. C. Yoo, C. Y. Heo, Y. B. Choy, *et al.*, Surgical suture releasing macrophage-targeted drug-loaded nanoparticles for an enhanced anti-inflammatory effect, *Biomater. Sci.*, 2017, **5**(8), 1670–1677.

2 H. Mohammadi, F. Alihosseini and S. A. Hosseini, Improving physical and biological properties of nylon monofilament as suture by Chitosan/Hyaluronic acid, *Int. J. Biol. Macromol.*, 2020, **164**, 3394–3402.

3 D. Sharma, S. Dhingra, A. Banerjee, S. Saha, J. Bhattacharyya and B. K. Satapathy, Designing suture-proof cell-attachable copolymer-mediated and curcumin-β-cyclodextrin inclusion complex loaded aliphatic polyester-based electrospun antibacterial constructs, *Int. J. Biol. Macromol.*, 2022, **216**, 397–413.

4 E. Altun, C. Bayram, M. Gultekinoglu, R. Matharu, A. Delbusso, S. Homer-Vanniasinkam, *et al.*, Pressure-Spun Fibrous Surgical Sutures for Localized Antibacterial Delivery: Development, Characterization, and In Vitro Evaluation, *ACS Appl. Mater. Interfaces*, 2023, **15**(39), 45561–45573.

5 S. Hasanpour, A. Rashidi, T. Walsh, E. Pagan, A. S. Milani, M. Akbari, *et al.*, Electrode-Integrated Textile-Based Sensors for In Situ Temperature and Relative Humidity Monitoring in Electrochemical Cells, *ACS Omega*, 2021, **6**(14), 9509–9519.

6 B. Mirani, E. Pagan, S. Shojaei, S. M. H. Dabiri, H. Savoji, M. Mehrali, *et al.*, Facile Method for Fabrication of Meter-Long Multifunctional Hydrogel Fibers with Controllable Biophysical and Biochemical Features, *ACS Appl. Mater. Interfaces*, 2020, **12**(8), 9080–9089.

7 L. Karperien, S. M. H. Dabiri, Z. Hadisi, D. Hamdi, E. Samiei and M. Akbari, Smart Thread Based pH Sensitive Antimicrobial Wound Dressing, IEEE International Flexible Electronics Technology Conference (IFETC), 2019.

8 P. Mostafalu, M. Akbari, K. A. Alberti, Q. Xu, A. Khademhosseini, S. R. Sonkusale, *et al.*, A toolkit of thread-based microfluidics, sensors, and electronics for 3D tissue embedding for medical diagnostics, *Microsyst. Nanoeng.*, 2016, **2**(1), 16039.

9 A. Fontana-Escartín, K. E. Hauadi, S. Lanzalaco, M. M. Pérez-Madrigal, E. Armelin, P. Turon, *et al.*, Smart Design of Sensor-Coated Surgical Sutures for Bacterial Infection Monitoring, *Macromol. Biosci.*, 2023, **23**(9), 2300024.

10 Y. Li, Q. Meng, S. Chen, P. Ling, M. A. Kuss, B. Duan, *et al.*, Advances, challenges, and prospects for surgical suture materials, *Acta Biomater.*, 2023, 78–112.

11 S. Fan, K. Chen, W. Yuan, D. Zhang, S. Yang, P. Lan, *et al.*, Biomaterial-Based Scaffolds as Antibacterial Suture Materials, *ACS Biomater. Sci. Eng.*, 2020, **6**(5), 3154–3161.

12 A. K. Narasimhan, T. S. Rahul and S. Krishnan, Revisiting the properties of suture materials: an overview, *Advanced Technologies and Polymer Materials for Surgical Sutures*, 2023.

13 C. Dennis, S. Sethu, S. Nayak, L. Mohan, Y. Y. Morsi and G. Manivasagam, Suture materials—Current and emerging trends, *J. Biomed. Mater. Res., Part A*, 2016, **104**(6), 1544–1559.

14 Y. Li, Q. Meng, S. Chen, P. Ling, M. A. Kuss, B. Duan and S. Wu, Advances, challenges, and prospects for surgical suture materials, *Acta Biomater.*, 2023, **168**, 78–112.

15 L. Xu, Y. Liu, W. Zhou, D. Yu, *et al.*, Electrospun Medical Sutures for Wound Healing: A Review, *Polymers*, 2022, **14**(9), 1637.

16 B. Joseph, A. George, S. Gopi, N. Kalarikkal and S. Thomas, Polymer sutures for simultaneous wound healing and drug delivery – A review, *Int. J. Pharm.*, 2017, 454–466.

17 R. H. Dong, C. C. Qin, X. Qiu, X. Yan, M. Yu, L. Cui, *et al.*, In situ precision electrospinning as an effective delivery technique for cyanoacrylate medical glue with high

efficiency and low toxicity, *Nanoscale*, 2015, **7**(46), 19468–19475.

18 C. Yang, Z. Jia, Z. Xu, K. Wang, Z. Guan and L. Wang, Comparisons of fibers properties between vertical and horizontal type electrospinning systems, 2009 IEEE Conference on Electrical Insulation and Dielectric Phenomena, 2009.

19 S. Suresh, A. Becker, B. Glasmacher, S. Suresh, A. Becker and B. Glasmacher, Impact of Apparatus Orientation and Gravity in Electrospinning—A Review of Empirical Evidence, *Polymers*, 2020, **12**(11), 2448.

20 M. Champeau, I. T. Coutinho, J. M. Thomassin, T. Tassaing and C. Jérôme, Tuning the release profile of ketoprofen from poly(L-lactic acid) suture using supercritical CO_2 impregnation process, *J. Drug Delivery Sci. Technol.*, 2020, **55**, 101468.

21 K. M. de la Harpe, T. Marimuthu, P. P. D. Kondiah, P. Kumar, P. Ubanako and Y. E. Choonara, Synthesis of a novel monofilament bioabsorbable suture for biomedical applications, *J. Biomed. Mater. Res., Part B*, 2022, **110**(10), 2189–2210.

22 H. Han, L. Tang, Y. Li, Y. Li, M. Bi, J. Wang, *et al.*, A multifunctional surgical suture with electroactivity assisted by oligochitosan/gelatin-tannic acid for promoting skin wound healing and controlling scar proliferation, *Carbohydr. Polym.*, 2023, **320**, 121236.

23 Y. Lee, H. Kim, Y. Kim, S. Noh, B. Chun, J. Kim, *et al.*, A multifunctional electronic suture for continuous strain monitoring and on-demand drug release, *Nanoscale*, 2021, **13**(43), 18112–18124.

24 A. S. Richard and R. S. Verma, Bioactive nano yarns as surgical sutures for wound healing, *Mater. Sci. Eng., C*, 2021, **128**, 112334.

25 Y. Ye, Y. Zhou, Z. Jing, Y. Xu and D. Yin, Electrospun heparin-loaded nano-fiber sutures for the amelioration of achilles tendon rupture regeneration: in vivo evaluation, *J. Mater. Chem. B*, 2021, **9**(20), 4154–4168.

26 M. J. Mochane, T. S. Motsoeneng, E. R. Sadiku, T. Clement Mokhena and J. S. Sefadi, Morphology and Properties of Electrospun PCL and Its Composites for Medical Applications: A Mini Review, *Applied Sciences*, 2019, **9**(11), 2205.

27 M. K. Alsaedi, R. E. Riccio, A. Sharma, J. Xia, R. E. Owyeung, L. M. Romero, *et al.*, Smart sensing flexible sutures for glucose monitoring in house sparrows, *Analyst*, 2023, **148**(22), 5714–5723.

28 A. M. Al-Enizi, M. M. Zagho, A. A. Elzatahry, A. M. Al-Enizi, M. M. Zagho and A. A. Elzatahry, Polymer-Based Electrospun Nanofibers for Biomedical Applications, *Nanomaterials*, 2018, **8**(4), 259.

29 R. S. Bhattarai, R. D. Bachu, S. H. S. Boddu, S. Bhaduri, R. S. Bhattarai, R. D. Bachu, *et al.*, Biomedical Applications of Electrospun Nanofibers: Drug and Nanoparticle Delivery, *Pharmaceutics*, 2019, **11**(1), 5.

30 S. Parham, A. Z. Kharazi, H. R. Bakhsheshi-Rad, H. Ghayour, A. F. Ismail, H. Nur, *et al.*, Electrospun Nano-Fibers for Biomedical and Tissue Engineering Applications: A Comprehensive Review, *Materials*, 2020, **13**(9), 2153.

31 X. Zhang, X. Shi, J. E. Gautrot and T. Peijs, Nanoengineered electrospun fibers and their biomedical applications: a review, *Nanocomposites*, 2021, **7**(1), 1–34.

32 R. J. Wade and J. A. Burdick, Advances in nanofibrous scaffolds for biomedical applications: From electrospinning to self-assembly, *Nano Today*, 2014, **9**(6), 722–742.

33 B. Lu, T. Li, H. Zhao, X. Li, C. Gao, S. Zhang, *et al.*, Graphene-based composite materials beneficial to wound healing, *Nanoscale*, 2012, **4**(9), 2978–2982.

34 L. Y. Long, W. Liu, L. Li, C. Hu, S. He, L. Lu, *et al.*, Dissolving microneedle-encapsulated drug-loaded nanoparticles and recombinant humanized collagen type III for the treatment of chronic wound via anti-inflammation and enhanced cell proliferation and angiogenesis, *Nanoscale*, 2022, **14**(4), 1285–1295.

35 M. Champeau, J. M. Thomassin, T. Tassaing and C. Jérôme, Current manufacturing processes of drug-eluting sutures, *Expert Opin. Drug Delivery*, 2017, 1293–1303.

36 Z. Sun, P. Huang, G. Tong, J. Lin, A. Jin, P. Rong, *et al.*, VEGF-loaded graphene oxide as theranostics for multimodality imaging-monitored targeting therapeutic angiogenesis of ischemic muscle, *Nanoscale*, 2013, **5**(15), 6857–6866.

37 F. C. Daoud, R. Goncalves and N. Moore, How Long Do Implanted Triclosan Sutures Inhibit *Staphylococcus aureus* in Surgical Conditions? A Pharmacological Model, *Pharmaceutics*, 2022, **14**(3), 539.

38 S. Sampathi, P. K. Tiriya, S. Dodoala, V. Junnuthula and S. Dyawanapelly, Development of Biocompatible Ciprofloxacin–Gold Nanoparticle Coated Sutures for Surgical Site Infections, *Pharmaceutics*, 2022, **14**(10).

39 Z. Yang, S. Liu, J. Li, G. Wu, M. Zhang, F. Li, *et al.*, Study on Preparation of Core-Spun Yarn Surgical Sutures by Compositing Drug-Loaded Nanofiber Membrane with PLA and Its Controllable Drug Release Performance, *Fibers Polym.*, 2023, **24**(12), 4181–4193.

40 T. H. Tseng, C. H. Chang, C. L. Chen, H. Chiang, H. Y. Hsieh, J. H. Wang, *et al.*, A simple method to improve the antibiotic elution profiles from polymethylmethacrylate bone cement spacers by using rapid absorbable sutures, *BMC Musculoskeletal Disord.*, 2022, **23**(1), 916.

41 D.-H. Kim, S. Wang, H. Keum, R. Ghaffari, Y.-S. Kim, H. Tao, *et al.*, Thin, Flexible Sensors and Actuators as 'Instrumented' Surgical Sutures for Targeted Wound Monitoring and Therapy, *Small*, 2012, **8**(21), 3263–3268.

42 M. Sriyai, J. Tasati, R. Molloy, P. Meepowpan, R. Somsunan, P. Worajittiphon, *et al.*, Development of an Antimicrobial-Coated Absorbable Monofilament Suture from a Medical-Grade Poly(L-lactide-co-ε-caprolactone) Copolymer, *ACS Omega*, 2021, **6**(43), 28788–28803.

43 E. Malikmammadov, T. Endogan Tanir, A. Kiziltay, V. Hasirci and N. Hasirci, PCL and PCL-based materials in biomedical applications, *J. Biomater. Sci., Polym. Ed.*, 2018, **29**(9), 863–893.

44 J. M. Hackett, T. T. Dang, E. C. Tsai and X. Cao, Electrospun Biocomposite Polycaprolactone/Collagen Tubes as Scaffolds for Neural Stem Cell Differentiation, *Materials*, 2010, **3**, 3714–3728.
45 D. J. Hines and D. L. Kaplan, Mechanisms of Controlled Release from Silk Fibroin Films, *Biomacromolecules*, 2011, **12**(3), 804–812.
46 S. Mohammadzadehmoghadam and Y. Dong, Fabrication and characterization of electrospun silk fibroin/gelatin scaffolds crosslinked with glutaraldehyde vapor, *Front. Mater.*, 2019, **6**, 454079.
47 M. Ebrahimi, S. Ostrovidov, S. Salehi, S. B. Kim, H. Bae and A. Khademhosseini, Enhanced skeletal muscle formation on microfluidic spun gelatin methacryloyl (GelMA) fibres using surface patterning and agrin treatment, *J. Tissue Eng. Regener. Med.*, 2018, **12**(11), 2151–2163.
48 C. J. Thompson, G. G. Chase, A. L. Yarin and D. H. Reneker, Effects of parameters on nanofiber diameter determined from electrospinning model, *Polymer*, 2007, **48**(23), 6913–6922.
49 T. Mazoochi, M. Hamadanian, M. Ahmadi and V. Jabbari, Investigation on the morphological characteristics of nanofiberous membrane as electrospun in the different processing parameters, *Int. J. Ind. Chem.*, 2012, **3**(1), 1–8.
50 A. Phongphut, C. Sriprachuabwong, A. Wisitsoraat, A. Tuantranont, S. Prichanont and P. Sritongkham, A disposable amperometric biosensor based on inkjet-printed Au/PEDOT-PSS nanocomposite for triglyceride determination, *Sens. Actuators, B*, 2013, **178**, 501–507.
51 M. Z. Çetin and P. Camurlu, An amperometric glucose biosensor based on PEDOT nanofibers, *RSC Adv.*, 2018, **8**(35), 19724–19731.
52 M. Kim, R. Iezzi, B. S. Shim and D. C. Martin, Impedimetric biosensors for detecting vascular endothelial growth factor (VEGF) based on poly(3,4-ethylene dioxythiophene) (PEDOT)/gold nanoparticle (Au NP) composites, *Front. Chem.*, 2019, **7**, 444510.
53 H. Bai, K. Vyshniakova, E. Pavlica, V. M. R. Malacco, A. Yiannikouris, T. R. Yerramreddy, *et al.*, Impedimetric, PEDOT:PSS-based organic electrochemical sensor for detection of histamine for precision animal agriculture, *IEEE Sens. Lett.*, 2020, **4**(10), 1–4.
54 I. M. Taylor, E. M. Robbins, K. A. Catt, P. A. Cody, C. L. Happe and X. T. Cui, Enhanced dopamine detection sensitivity by PEDOT/graphene oxide coating on in vivo carbon fiber electrodes, *Biosens. Bioelectron.*, 2017, **89**, 400–410.
55 N. Chauhan, S. Chawla, C. S. Pundir and U. Jain, An electrochemical sensor for detection of neurotransmitter-acetylcholine using metal nanoparticles, 2D material and conducting polymer modified electrode, *Biosens. Bioelectron.*, 2017, **89**, 377–383.
56 B. Bessaire, M. Mathieu, V. Salles, T. Yeghoyan, C. Celle, J. P. Simonato, *et al.*, Synthesis of continuous conductive PEDOT:PSS nanofibers by electrospinning: A conformal coating for optoelectronics, *ACS Appl. Mater. Interfaces*, 2017, **9**(1), 950–957.
57 V. Dini, P. Salvo, A. Janowska, F. Di Francesco, A. Barbini and M. Romanelli, Correlation Between Wound Temperature Obtained With an Infrared Camera and Clinical Wound Bed Score in Venous Leg Ulcers, *Wounds*, 2015, **27**(10), 274–278.
58 A. C. B. Allen, E. Barone, C. O. Crosby, L. J. Suggs and J. Zoldan, Electrospun poly(N-isopropyl acrylamide)/poly (caprolactone) fibers for the generation of anisotropic cell sheets, *Biomater. Sci.*, 2017, **5**(8), 1661–1669.
59 T. Tran, M. Hernandez, D. Patel, E. Burns, V. Peterman and J. Wu, Controllable and switchable drug delivery of ibuprofen from temperature responsive composite nanofibers, *Nano Convergence*, 2015, **2**(15), 1–7.
60 Z. Hadisi, J. Nourmohammadi and S. M. Nassiri, The antibacterial and anti-inflammatory investigation of Lawsonia Inermis-gelatin-starch nano-fibrous dressing in burn wound, *Int. J. Biol. Macromol.*, 2018, **107**, 2008–2019.
61 S. F. Chou, D. Carson and K. A. Woodrow, Current strategies for sustaining drug release from electrospun nanofibers, *J. Controlled Release*, 2015, **220**, 584–591.
62 J. Kopp, G. Y. Wang, P. Kulmburg, S. Schultze-Mosgau, J. N. Huan, K. Ying, *et al.*, Accelerated wound healing by in vivo application of keratinocytes overexpressing KGF, *Mol. Ther.*, 2004, **10**, 86–96.
63 L. Meinel, S. Hofmann, V. Karageorgiou, C. Kirker-Head, *et al.*, The inflammatory responses to silk films in vitro and in vivo, *Biomaterials*, 2005, **26**(2), 147–155.
64 S.-C. Wu, W.-H. Chang, G.-C. Dong, K.-Y. Chen, Y.-S. Chen and C.-H. Yao, Cell adhesion and proliferation enhancement by gelatin nanofiber scaffolds, *J. Bioact. Compat. Polym.*, 2011, **26**(6), 565–577.
65 J. L. Ferreira, S. Gomes, C. Henriques, J. P. Borges and J. C. Silva, Electrospinning polycaprolactone dissolved in glacial acetic acid: Fiber production, nonwoven characterization, and In Vitro evaluation, *J. Appl. Polym. Sci.*, 2014, **131**(22), 41068.
66 D. Mondal, M. Griffith and S. S. Venkatraman, Polycaprolactone-based biomaterials for tissue engineering and drug delivery: Current scenario and challenges, *Int. J. Polym. Mater. Polym. Biomater.*, 2016, **65**(5), 255–265.
67 M. Gabriel, G. P. van Nieuw Amerongen, V. W. M. Van Hinsbergh, A. V. Van Nieuw Amerongen and A. Zentner, Direct grafting of RGD-motif-containing peptide on the surface of polycaprolactone films, *J. Biomater. Sci., Polym. Ed.*, 2006, **17**(5), 567–577.
68 A. S. Badami, M. R. Kreke, M. S. Thompson, J. S. Riffle and A. S. Goldstein, Effect of fiber diameter on spreading, proliferation, and differentiation of osteoblastic cells on electrospun poly(lactic acid) substrates, *Biomaterials*, 2006, **27**(4), 596–606.
69 B. M. Min, G. Lee, S. H. Kim, Y. S. Nam, T. S. Lee, W. H. Park, *et al.*, Electrospinning of silk fibroin nanofibers and its effect on the adhesion and spreading of normal human keratinocytes and fibroblasts in vitro, *Biomaterials*, 2004, **25**(7), 1289–1297.
70 C. Y. Huang, K. H. Hu and Z. H. Wei, Comparison of cell behavior on PVA/PVA-gelatin electrospun nanofibers with

random and aligned configuration, *Sci. Rep.*, 2016, **6**, 37960.

71 X. Wang, P. Liu, Q. Wu, Z. Zheng, M. Xie, G. Chen, *et al.*, Sustainable Antibacterial and Anti-Inflammatory Silk Suture with Surface Modification of Combined-Therapy Drugs for Surgical Site Infection, *ACS Appl. Mater. Interfaces*, 2022, **14**(9), 11177–11191.

72 A. Dasgupta, N. Sori, S. Petrova, Y. Maghdouri-White, N. Thayer, N. Kemper, *et al.*, Comprehensive collagen cross-linking comparison of microfluidic wet-extruded microfibers for bioactive surgical suture development, *Acta Biomater.*, 2021, **128**, 186–200.

73 X. Deng, M. Gould and M. A. Ali, Fabrication and characterisation of melt-extruded chitosan/keratin/PCL/PEG drug-eluting sutures designed for wound healing, *Mater. Sci. Eng., C*, 2021, **120**, 111696.

74 D. Sharma and B. K. Satapathy, Understanding release kinetics and collapse proof suture retention response of curcumin loaded electrospun mats based on aliphatic polyesters and their blends, *J. Mech. Behav. Biomed. Mater.*, 2021, **120**, 104556.

75 Z. Hadisi, J. Nourmohammadi and J. Mohammadi, Composite of porous starch-silk fibroin nanofiber-calcium phosphate for bone regeneration, *Ceram. Int.*, 2015, **41**(9), 10745–10754.

76 C. Brooker and G. Tronci, A collagen-based theranostic wound dressing with visual, long-lasting infection detection capability, *Int. J. Biol. Macromol.*, 2023, **236**, 123866.